


Nutritional response of a coccolithophore to changing pH and temperature

Roberta Johnson ^{1,*}, Gerald Langer,¹ Sergio Rossi,^{1,2} Ian Probert,³ Marta Mammone,² Patrizia Ziveri^{1,4}

¹Institut de Ciència i Tecnologia Ambientals, Universitat Autònoma de Barcelona, Barcelona, Spain

²Department of Biological and Environmental Sciences and Technologies, University of Salento, Lecce, Italy

³Sorbonne Université, CNRS, Roscoff Culture Collection, Station Biologique de Roscoff, Roscoff, France

⁴Institució Catalana de Recerca i Estudis Avançats (ICREA), Barcelona, Spain

Abstract

Coccolithophores are a calcifying unicellular phytoplankton group that are at the base of the marine food web, and their lipid content provides a source of energy to consumers. Coccolithophores are vulnerable to ocean acidification and warming, therefore it is critical to establish the effects of climate change on these significant marine primary producers, and determine potential consequences that these changes can have on their consumers. Here, we quantified the impact of changes in pH and temperature on the nutritional condition (lipid content, particulate organic carbon/nitrogen), growth rate, and morphology of the most abundant living coccolithophore species, *Emiliana huxleyi*. We used a regression type approach with nine pH levels (ranging from 7.66 to 8.44) and two temperatures (15°C and 20°C). Lipid production was greater under reduced pH, and growth rates were distinctly lower at 15°C than at 20°C. The production potential of lipids, which estimates the availability of lipids to consumers, increased under 20°C, but decreased under low pH. The results indicate that, while consumers will benefit energetically under ocean warming, this benefit will be mitigated by ocean acidification. The carbon to nitrogen ratio was higher at 20°C and low pH, indicating that the nutritional quality of coccolithophores for consumers will decline under climate change. The impact of low pH on the structural integrity of the coccosphere may also mean that coccolithophores are easier to digest for consumers. Many responses suggest cellular stress, indicating that increases in temperature and reductions in pH may have a negative impact on the ecophysiology of coccolithophores.

Coccolithophores are unicellular calcifying phytoplankton found in all of the world's oceans. They influence seawater chemistry and the exchange of carbon dioxide between the atmosphere and the ocean via photosynthesis and the

formation and dissolution of their calcium carbonate skeleton. An estimated 83% of the organic carbon flux to the seafloor is associated with their calcium carbonate ballast (Klaas and Archer 2002), establishing coccolithophores as major contributors to the carbon cycle in the oceans (Ziveri et al. 2007; Falkowski et al. 2008; Lefebvre et al. 2011).

Coccolithophores form part of the base of the food web, and their nutritional quality, particularly in terms of their organic carbon to nitrogen ratio and lipid content, are important predictors of the nutritional condition for consumers at higher trophic levels (Pond and Harris 1996; Mitra and Flynn 2005; Schlüter et al. 2014). In phytoplankton, lipids (total and fatty acids) serve as structural molecules within cells and as energy storage units (Fuentes-Grünwald et al. 2012). These are key determinants of food quality, and, in turn, the health and functioning of marine ecosystems (Jin et al. 2020). Chlorophyll *a* (Chl *a*), an indicator of photosynthetic capacity, contains a large amount of lipids, and, as such, increases in Chl *a* are usually associated with an increase in lipids (Woodworth et al. 2015) as well as photosynthetic performance. These lipid macromolecules provide a source of energy

*Correspondence: roberta.johnson@uab.cat

This is an open access article under the terms of the [Creative Commons Attribution-NonCommercial](https://creativecommons.org/licenses/by-nc/4.0/) License, which permits use, distribution and reproduction in any medium, provided the original work is properly cited and is not used for commercial purposes.

Additional Supporting Information may be found in the online version of this article.

Author Contribution Statement: R.J. conducted the experiment, analyzed the carbonate chemistry data, the morphological data, performed the statistical analyses, and drafted the manuscript. G.L. assisted with the experiment and experimental design and assisted with writing the manuscript. S.R. analyzed the lipid samples, assisted with writing the manuscript, and created the original concept. I.P. assisted with the experiment, and with writing the manuscript. M.M. analyzed the chlorophyll *a* samples, the carbon and nitrogen samples, and assisted with writing the manuscript. P.Z. assisted with the experimental design, writing the manuscript, conceptualization, resources, and supervision.

to phytoplankton consumers higher on the trophic ladder (Broglio et al. 2003; Litzow 2006), and changes in the availability of essential fatty acids can have a significant impact on consumer productivity (Fraser et al. 1989; Breteler et al. 2005). Suspension feeders and zooplankton depend on primary producers as a food source (Sailley et al. 2013; El-Hady et al. 2016), and food quality and availability is a major factor affecting reproduction and survival in these organisms (Gili and Coma 1998; Broglio et al. 2003; Gori et al. 2013).

Any detrimental effects of climate change on phytoplankton physiology may have cascading effects on other components of the ecosystem (Chavez et al. 2010; Guinder and Molinero 2013). For instance, increased $p\text{CO}_2$ has been shown to effect trophic transfer efficiency between phytoplankton and their consumer, copepod *Acartia tonsa* (Cripps et al. 2016). In addition, four species of phytoplankton grown under high CO_2 conditions (1000 ppm) showed reduced essential fatty acid content, and the copepods consuming this plankton experienced reduced egg production, hatching success, and egg viability (Meyers et al. 2019). The diatom *Thalassiosira pseudonana* experienced reduced fatty acid content under elevated $p\text{CO}_2$, which translated to a 10-fold decrease in fatty acids for the consumer, copepod *A. tonsa*, including a decrease in somatic growth and egg production from 34 to 5 eggs female⁻¹ d⁻¹ (Rossoll et al. 2012). When considering such drastic impacts that changes in phytoplankton nutritional status can have on consumers, it is critical to establish the effects of climate change stressors on this significant marine phytoplankton, and the consequences that they may have on the food web (Rossi et al. 2019).

Emiliania huxleyi is one of the most abundant coccolithophores in the oceans and is responsible for giant seasonal algal blooms (Brown and Yoder 1994) that are visible from space (Holligan et al. 1993). Such blooms can provide a substantial food source to zooplankton grazers (Pond and Harris 1996). *E. huxleyi* is known to produce stable lipid compounds, including alkenones, alkyl alkenones, and alkenes, which can be used as climatic proxies to evaluate the impacts of a changing climate (Bendle et al. 2005; Malinverno et al. 2008). *E. huxleyi* has been studied extensively and found to be sensitive to ocean acidification conditions (Riebesell et al. 2000; Beaufort et al. 2011; Lefebvre et al. 2011; Schlüter et al. 2014). The most relevant climate change impacts for coccolithophores are ocean acidification and ocean warming.

Ocean acidification is the result of increasing atmospheric CO_2 , which is absorbed by the ocean, resulting in an increase in $[\text{H}^+]$ and a decrease in ocean pH, as well as a decrease in the concentration of carbonate ions (Fabry et al. 2008; Doney et al. 2009). Global open ocean surface seawater pH is projected to decrease by approximately 0.3 units by 2100 under RCP 8.5 (business as usual scenario; IPCC 2019). The reduction in seawater pH has been shown to impact *E. huxleyi* calcification (Riebesell et al. 2000; Lefebvre et al. 2011; Schlüter et al. 2014), morphology (Langer et al. 2009; Lefebvre et al. 2011),

photosynthetic ability (Bach et al. 2013; Fukuda et al. 2014), and growth rate (Lefebvre et al. 2011; Bach et al. 2013; Schlüter et al. 2014).

Global sea surface temperature is expected to increase by approximately 3°C on average by the end of this century, though this will vary by region (RCP 8.5; IPCC 2019). Ocean warming has been shown to impact coccolithophore growth (Schlüter et al. 2014; Rosas-Navarro et al. 2016; Feng et al. 2017; Krumhardt et al. 2017), calcification (Rosas-Navarro et al. 2016; Feng et al. 2017; Krumhardt et al. 2017), and morphology (Rosas-Navarro et al. 2016). The combined impacts of ocean acidification and warming have also been shown to have an interactive effect on coccolithophore growth (Arnold et al. 2013; Sett et al. 2014; D'Amario et al. 2017), morphology (Milner et al. 2016; D'Amario et al. 2017), calcification (Schlüter et al. 2014; Sett et al. 2014), and photosynthesis (Sett et al. 2014).

Although there has been some focus on the effects of climate change stressors on the quality of some primary producers as a food source (Klauschie et al. 2012; Guinder and Molinero 2013), there has been no published work that investigates how ocean acidification combined with ocean warming conditions will alter the quality and quantity (in terms of food availability) of coccolithophores as a source of nutrition for higher trophic levels. This study aims to fill this gap. We focus on *E. huxleyi* here due to its extensive use in previous studies, making this an ideal species for comparison. The hypothesis tested here is that reduced pH (in line with ocean acidification) and increased temperature (ocean warming) will likely affect the quality of coccolithophores as a food source (Guinder and Molinero 2013) by impacting their investment in stored energy (in the form of lipids). This is investigated here by measuring cellular lipid content (Pond and Harris 1996), as well as carbon and nitrogen ratios. We also explore the impact of pH and temperature on food quantity through a parameter known as production potential, which combines cell growth with cellular lipid content. Production potential translates cellular lipid production to community production and estimates the availability of lipids in a coccolithophore community (Gafar et al. 2018; Klintzsch et al. 2019). These points have rarely been addressed, particularly in a combined ocean acidification and warming scenario. In addition, we investigate the impacts of pH and temperature on important parameters related to coccolithophore nutritional quality, including growth rate, particulate organic and inorganic content, and coccosphere morphology (Table 1).

Materials and methods

Culture medium preparation

Seawater collected from 3 km off the coast of Roscoff (Brittany, France) on the 3rd and 10th of June 2019 was mixed homogeneously, pre-filtered using 0.7- μm nominal pore size

Table 1. Information on how each response variable relates to nutritional quantity or quality, and other parameters indicating fitness and cellular function for *Emiliania huxleyi*. The response variables include: lipids (pg cell⁻¹), POC (pg cell⁻¹), PIC (pg cell⁻¹), Chl *a* (pg cell⁻¹), growth rate (day⁻¹), lipid production (pg cell⁻¹ d⁻¹), POC production (pg cell⁻¹ d⁻¹), PIC production (pg cell⁻¹ d⁻¹), Chl *a* production (pg cell⁻¹ d⁻¹), production potential—lipids (ng), POC : N, PIC : N, PIC : POC, lipid : POC (cellular lipid content : cellular POC content), coccosphere diameter (μm), coccolith distal shield length (μm), coccolith distal shield width (μm), inner circle diameter (μm), tube width (μm), collapsed coccosphere (%).

| Response variable | Parameter relevance |
|--------------------------------------|--|
| Cellular quotas | |
| Lipid quota | High-energy carbon source Increase indicates higher associated energy to catabolize (food quantity) |
| POC quota | Organically digestible carbon—comprised of both low and high energy (i.e., lipids) compounds |
| PIC quota | Increase might indicate lower food quality |
| Chl <i>a</i> quota | Increase can indicate higher capability of photosynthesis—effect on food quality uncertain |
| Production rates | |
| Growth rate | Main driver of food production (quantity) |
| Lipid production | Food quantity (energy) production Note that this is cellular level and less important for consumers (see also production potential) |
| POC production | Food quantity (see also production potential) Alone insufficient to indicate food quality |
| PIC production | Increase tends to lower food quality but ratios more informative |
| Chl <i>a</i> production | Effect on food quality/quantity uncertain |
| Production potential—lipids | Best indication of food quantity for coccolithophore consumers Amount of lipids available to consumers after a given period of growth |
| Carbon ratios | |
| POC : N | High-quality food (low ratio), that is, less nitrogen Nitrogen is involved in the production of amino acids and proteins, including chlorophyll, and is essential for cellular function |
| PIC : N | High food quality (low ratio) PIC has no nutritional value but might hamper digestion |
| PIC : POC | High food quality (low ratio), that is, less PIC |
| Lipid : POC | High food quality (high ratio), that is, more lipids |
| Morphological characteristics | |
| Coccosphere diameter | Reduced size may mean the coccosphere is more easily digestible for nonselective grazers |
| Distal shield length | General coccolith morphological parameter—differences indicate change in growth and/or calcification |
| Distal shield width | General coccolith morphological parameter—differences indicate change in growth and/or calcification |
| Inner circle diameter | General coccolith morphological parameter—differences indicate change in growth and/or calcification |
| Tube width | General coccolith morphological parameter—differences indicate change in growth and/or calcification |
| Collapsed coccospheres | Weak coccospheres may mean cell contents are more readily digestible for selective grazers |

glass fiber filters (Whatman GF/F) and 0.2-μm mixed cellulose ester membrane filters (Millipore), heated to 80°C for 10 min, and then cooled overnight. The seawater was enriched with 100 μmol L⁻¹ nitrate, 6.25 μmol L⁻¹ phosphate, trace metals, and vitamins as in K/2 medium (Keller et al. 1987). The culture medium was then filter sterilized using 0.2 μm Fast Flow Polyethersulfone (PES) Express PLUS filter modules (Millipore).

Cultures of *E. huxleyi* RCC 1832 (Western Mediterranean strain collected from latitude 39°10'N and longitude 5°35'E; Type A morphotype) from the Roscoff Culture Collection (www.roscoff-culture-collection.org) were initially grown for 1 week at a light intensity of 150 μmol m⁻² s⁻¹ in a 16/8 h

light/dark cycle in culture cabinets set to either 15°C or 20°C. Using these initial temperature acclimated pre-cultures, acclimation cultures were inoculated with 500 cells mL⁻¹ in culture flasks (300 mL) and held in experimental conditions (two temperatures: 15°C and 20°C, 9 pH levels targeted to approximately: 8.4, 8.3, 8.2, 8.1, 8.0, 7.9, 7.8, 7.7, 7.6, light regime as above) until cell concentrations reached between 50,000 and 100,000 cells mL⁻¹. For the experimental cultures, polycarbonate Nalgene bottles (2.95 liter) completely filled with sterile culture medium with target pH levels (refer to “Carbonate system” section) were then inoculated with either 500, 1000, or 2000 cells mL⁻¹ from the corresponding acclimation culture, and incubated in the same temperature

and light conditions as the acclimation cultures (without replication). Experimental cultures were sampled for the response variables once cell counts reached approximately 50,000–100,000 cells mL⁻¹. This so-called dilute batch approach ensures a quasi-constant seawater carbonate chemistry (Langer et al. 2009).

As a western Mediterranean Sea strain of *E. huxleyi* was used here, the temperature levels were chosen to reflect current and future projected temperatures for this region. The optimum growth temperature for this strain is likely within the range of 22–25°C based on other strains of *E. huxleyi* collected from the western Mediterranean Sea. The higher temperature of 20°C was chosen to ensure that thermal damage to lipids and proteins did not occur, and that the cultures did not crash, particularly as the combined, and possible synergistic, effect of temperature and pH was not known. This is particularly important when investigating the impact of multiple stressors, as reduced pH and increased temperature are known to have negative interactive effects on multiple physiological parameters for coccolithophores (Arnold et al. 2013; Sett et al. 2014; D'Amario et al. 2017). In the Algerian Basin, where this culture originated from, recorded sea surface temperatures range from 14°C to 16°C in winter, 18°C to 18.4°C in spring (for 80% of the basin), 19.5°C to 19.9°C in autumn (for 50% of the basin), and 24.5°C to 24.9°C in summer (for 70% of the basin; Shaltout and Omstedt 2014). Anticipating a 3°C warming of sea surface temperatures by 2100, 20°C is a useful temperature to investigate the potential impacts of ocean warming, as by 2100, average temperatures in the region that this strain of *E. huxleyi* was collected will be closer to 20°C for most of the year. A 5°C difference between temperatures was chosen to ensure a clear, observable effect (if there was one) of temperature on the response variables.

We utilized a large range of pH levels (ranging from 7.66 to 8.44) and two temperatures (15°C and 20°C) to create a response curve for the dependent variables over the two temperature levels. The lower end of the pH range is in line with, and exceeds, future predictions of ocean acidification over the next century, the middle range is in line with current ocean pH levels, and the upper range includes preindustrial pH levels and above. A higher number of treatment levels for pH were used at the expense of replication and a generalized linear model (GLM) including linear and nonlinear terms was used to analyze the data (Cottingham et al. 2005).

Growth rates

Cell counts were conducted using a Guava easyCyte HT flow cytometer (software guavaSoft 3.1.1—detected via chlorophyll fluorescence) at the same time each day (after cell counts were estimated to be above 4000 cells mL⁻¹). Cells were suspended in the Nalgene bottles to ensure cell concentrations were homogenous by inverting the bottle 5–10 times. Cell counts were conducted in duplicate (200 μL). The Nalgene bottle lids were covered in parafilm between each sampling to

minimize gas exchange. Cell growth rates were determined using the equation $growth\ rate = [\ln(D_f) - \ln(D_0)]/t$, where D_f is the final concentration, D_0 is the initial concentration, and t is the time in days. At the end of the experiment, all samples were taken within 3 h of conducting cell counts.

Lipids

For total lipid extraction, triplicate 0.15 liter samples were filtered onto precombusted (8 h, 450°C) GF/F Whatman glass-fiber filters, immediately frozen in liquid N₂ and then stored at -20°C until analysis. Lipids were extracted in chloroform : methanol (2 : 1) following Barnes and Blackstock (1973) (colorimetry). Samples were evaporated and sulfuric acid was added; the final reaction was performed using vanillin. Cholesterol was used as a standard, and measurements were read using a spectrophotometer (UV mini1240, Shimadzu). Lipid cellular quotas are reported as pg cell⁻¹. The production rate for lipids (pg cell⁻¹ d⁻¹) was calculated as:

$$\text{Lipid production} = \text{growth rate} \times \text{cellular lipid content pg cell}^{-1}.$$

Production potential is a parameter that extrapolates the cellular lipid production of a community of coccolithophores. This parameter assumes exponential growth and starts from a known cell density (1 cell). The corresponding lipid production of the community can be calculated using the growth rate (μ) and cellular lipid content (pg cell⁻¹) to determine the amount of lipids available to consumers after 1 week of growth (Gafar et al. 2018; Klintzsch et al. 2019). The following equation was used to calculate the production potential of lipids:

$$PP_{\text{lipids}} = N_0 \times e^{\mu \times t} \times \frac{m(\text{lipids})}{\text{cell}},$$

where PP_{lipids} is the production potential of lipids after 7 d, N_0 is the assumed cell density of the community (using a starting cell density of 1), e is the exponential growth factor, μ is the growth rate, t is the time in days (here we use 7 d), m (lipids) is the cellular lipid content (pg cell⁻¹) of each experimental culture, and $cell$ is the final cell concentration.

Particulate inorganic/organic carbon and nitrogen ratios

For the determination of total particulate carbon (TPC includes both inorganic and organic carbon; duplicates) and particulate organic carbon (POC; duplicates), 0.25 liter of water was filtered onto precombusted (8 h, 450°C) 0.7-μm nominal pore size glass fiber filters (Whatman GF/F) and stored at -20°C. The filters for POC analysis were dried at 60°C for 24 h, then exposed to HCl vapors for 48 h to dissolve the calcite and convert all particulate inorganic carbon (PIC) to CO₂, leaving only POC to be measured (Rossi and Gili 2007). These filters were then redried at 60°C for 24 h. The analyses were performed with an elemental analyzer

(Elementar Vario Pyro Cube EA CNS; Elementar Analysensysteme GmbH, Hanau, Germany). To calculate PIC, which represents the calcite shell of the coccolithophore, POC was subtracted from TPC. PIC and POC (pg cell^{-1}) were calculated as well as C : N ratios (particulate inorganic or organic carbon : nitrogen).

Rates of production for particulate inorganic carbon ($\text{pg cell}^{-1} \text{d}^{-1}$) and particulate organic carbon ($\text{pg cell}^{-1} \text{d}^{-1}$) were calculated as:

$$\text{PIC production} = \text{growth rate} \times \text{PIC content } \text{pg cell}^{-1},$$

and

$$\text{POC production} = \text{growth rate} \times \text{POC content } \text{pg cell}^{-1}.$$

The ratio between lipids (pg cell^{-1}) and POC (pg cell^{-1}) was used to explore the relationship between cellular lipids and POC content ($\text{lipid} : \text{POC} \times 100$).

Chlorophyll *a*

To determine the Chl *a* concentration, 3×100 mL replicates were filtered through GF/F precombusted glass fiber filters and stored at -20°C . Chlorophyll was extracted in 8 mL 90% acetone and left for 24 h covered with aluminum foil at $+4^\circ\text{C}$. Samples were then centrifuged for 15 min at 10,000g and 4°C , and then analyzed using a spectrophotometer (UV mini1240, Shimadzu). The absorbance was read at 630, 663, and 750 nm. Chl *a* concentration was calculated according to the spectrometric equations reported in Jeffrey and Humphrey (1975). Chl *a* cellular quotas are reported as pg cell^{-1} . The production rate for Chl *a* ($\text{pg cell}^{-1} \text{d}^{-1}$) was calculated as:

$$\text{Chl } a \text{ production} = \text{growth rate} \\ \times \text{cellular Chl } a \text{ content } \text{pg cell}^{-1}.$$

Morphology

Malformations in coccolith formation might lead to unstable coccospheres, which in turn may lead to impaired protection (Monteiro et al. 2016; Kottmeier et al. 2022). To investigate potential malformation, 1 mL samples for scanning electron microscopy were filtered onto $0.8\text{-}\mu\text{m}$ pore size polycarbonate filters (Millipore) and dried in a drying cabinet at 55°C for 24–48 h. A desktop Phenom G2 pro scanning electron microscope was used to take images for subsequent analysis (using ImageJ software) of coccosphere diameter (along the longest axis) and coccolith morphological features (distal shield length, distal shield width, inner circle diameter, tube width; Supporting Information Fig. S1).

To determine whether the integrity of the coccolithophore cell was maintained, cell counts of collapsed (four or more

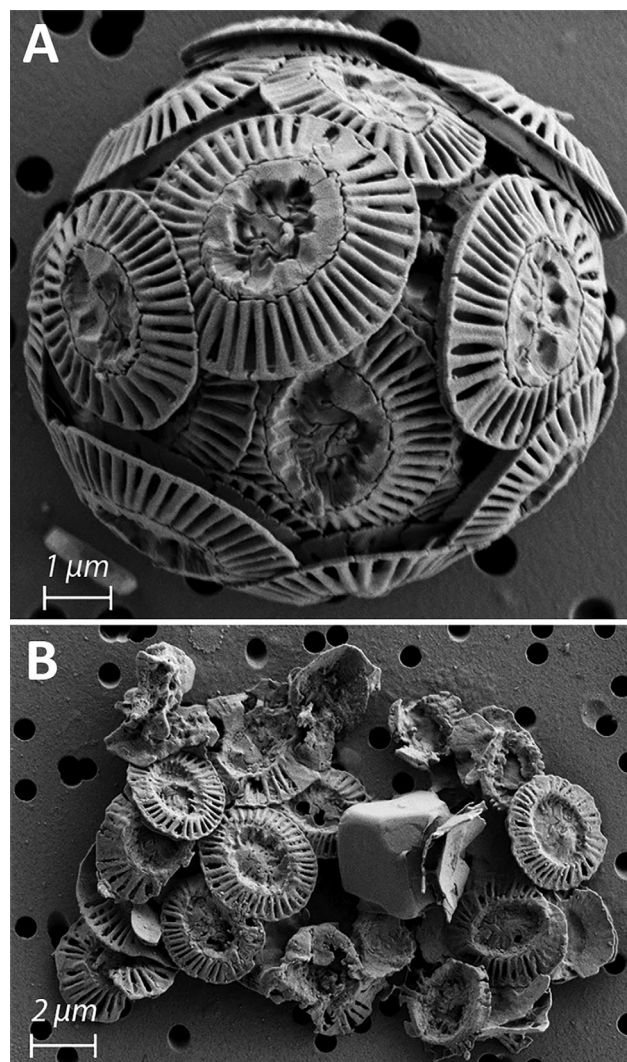


Fig. 1. (A) An intact coccosphere and (B) a collapsed coccosphere of *Emiliana huxleyi*. Images taken using a desktop Phenom G2 pro scanning electron microscope.

interlocked coccoliths; Fig. 1) and intact coccospheres (Fig. 1) were conducted using a scanning electron microscope (Merlin, Zeiss). The results are reported as a percentage of the total cell count.

Carbonate system

The pH of experimental cultures was adjusted through calculated additions of either HCl or NaOH. Samples for total alkalinity (TA) were collected from the filtrate of the TPC/POC filters and stored at 4°C for a maximum of 7 d before processing. The TA was measured in duplicates via titration with Metrohm 877 Titrino plus (software tiBase 1.1) at 25°C using Dickson Certified Standards (Batch #100).

Samples for pH were collected using unfiltered experimental medium and stored in gas tight bottles, without air bubbles. All samples were measured spectrophotometrically in

triplicate within 3 h of collection in the method of Liu et al. (2011) at 25°C (PerkinElmer UV/VIS Lambda 365).

The carbonate system was calculated with TA and pH using CO2SYS (Pierrot et al. 2011). The TA and pH were measured at 25°C and used to calculate DIC. Following this, TA and DIC were used to calculate the system at the target temperature (either 15°C or 20°C; Supporting Information Table S1).

Statistics

Data were analyzed using a GLM (Nelder and Wedderburn 1972; Zuur et al. 2009a). Each model was run using a gamma distribution with log link (continuous response variable Y that has positive values >0 ; Zuur et al. 2009b), and chosen following a backward selection criteria and based on the lowest Akaike information criterion (AIC) score (Aho et al. 2014). In the model, temperature was selected as the fixed factor and pH as the co-variate, including their interaction and possible nonlinear responses (with a maximum nonlinearity of a cubic term— pH^3). Significant variables ($p < 0.05$) for the chosen models were included. Only significant terms were kept in the model except in instances where models including nonsignificant variables had lower AIC scores. The following linear and nonlinear predictors were tested in the GLM:

$$\text{Response variable} \sim \text{temperature} + \text{pH} + \text{pH}^2 + \text{pH}^3 + \text{temperature} * \text{pH}.$$

The model was run with 100 iterations and Wald chi-squared statistics and confidence intervals were used. For the covariance matrix, the robust estimate was used which provides a more conservative model. A Type III analysis was chosen as it holds all the variables constant relative to each other. Data from each sample were averaged to create a single data point for each treatment. Assumptions of normality were satisfied for each dependent variable (Shapiro–Wilk test). Outliers were defined as any data point outside of the following ranges— 3^{rd} quartile + $1.5 * \text{interquartile range}$ or 1^{st} quartile— $1.5 * \text{interquartile range}$, and were removed from the dataset for the statistical analysis. The reference category is included for comparison against the other predictors. The models were run using IBM SPSS v22. The GLM results are reported in detail in the Supporting Information (Table S2).

Results

Cellular quotas

The average cellular lipid content for both temperatures across all pH levels was $44.75 \text{ pg cell}^{-1}$ (SD = 9.25;

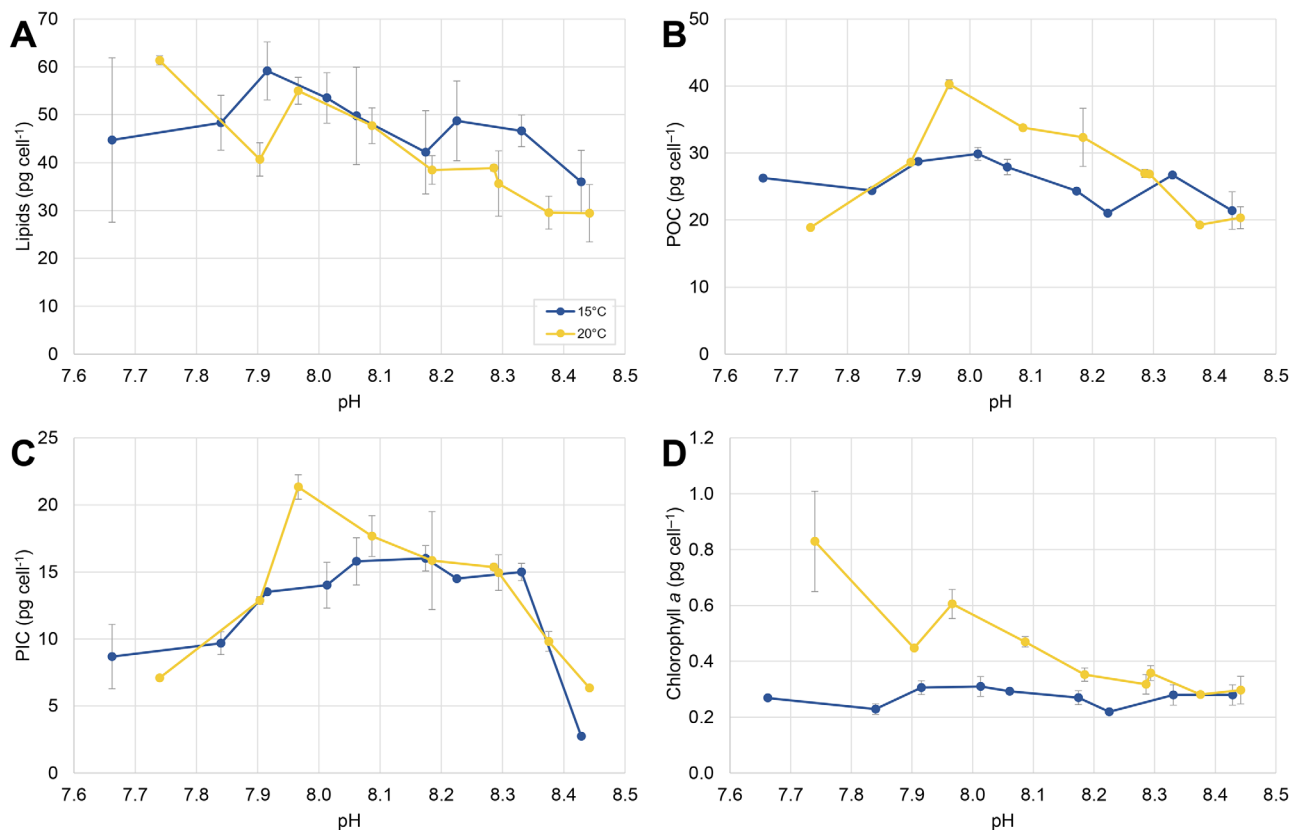


Fig. 2. Cellular quotas in response to pH levels and temperatures. (A) Lipids (pg cell^{-1}), (B) POC (pg cell^{-1}), (C) PIC (pg cell^{-1}), and (D) Chl a (pg cell^{-1}). Error bars indicate data standard deviation within each treatment, not between replicates.

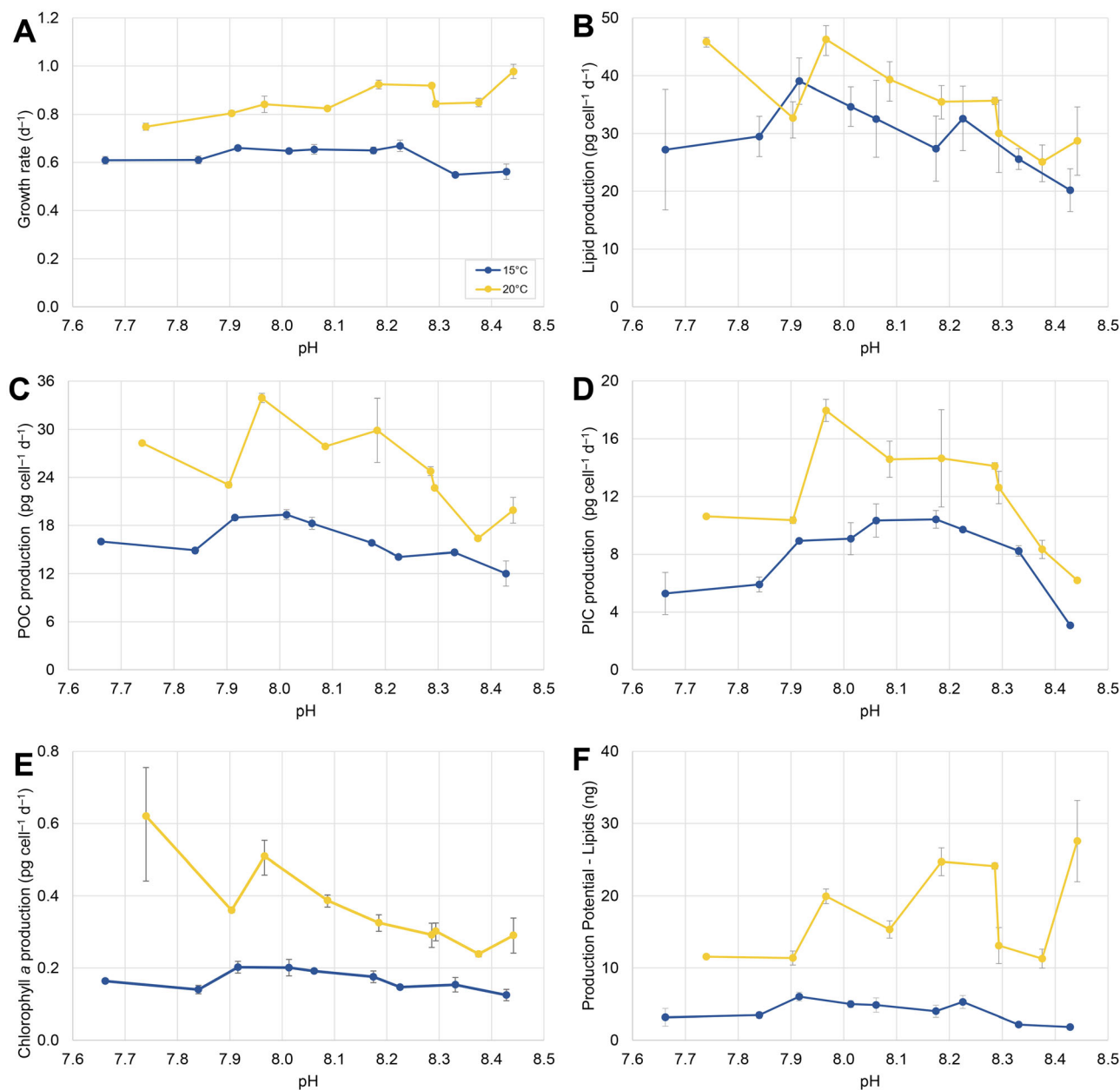


Fig. 3. Production rates in response to pH levels and temperatures. **(A)** Growth rate (day⁻¹), **(B)** lipid production (pg cell⁻¹ d⁻¹), **(C)** POC production (pg cell⁻¹ d⁻¹), **(D)** PIC production (pg cell⁻¹ d⁻¹), **(E)** Chl *a* production (pg cell⁻¹ d⁻¹), and **(F)** production potential—lipids (ng). Error bars indicate data standard deviation within each treatment, not between replicates.

range = 29.42–61.34 pg cell⁻¹). The average cellular lipid content at 15°C (47.66 pg cell⁻¹; SD = 6.61) was slightly higher than at 20°C (41.85 pg cell⁻¹; SD = 10.92). Cellular lipid content increased as pH decreased and this trend appeared to be similar across both temperatures (Fig. 2A). The quadratic term for pH was significant in the selected model (Supporting Information Table S2). Temperature, pH, and their interaction were significant predictors for cellular lipid content (Supporting Information Table S2).

Cellular POC content (pg cell⁻¹) followed a parabolic trend at 20°C (Fig. 2B), with a higher average of 27.50 pg cell⁻¹ (SD = 7.25) than at 15°C (25.64 pg cell⁻¹; SD = 3.10). At 15°C, cellular POC content had a linear trend, which slightly decreased toward higher pH (Fig. 2B). The selected model includes a significant quadratic term for pH (Supporting Information Table S2). Temperature was not a significant predictor yet is still included in the model (lowest AIC value).

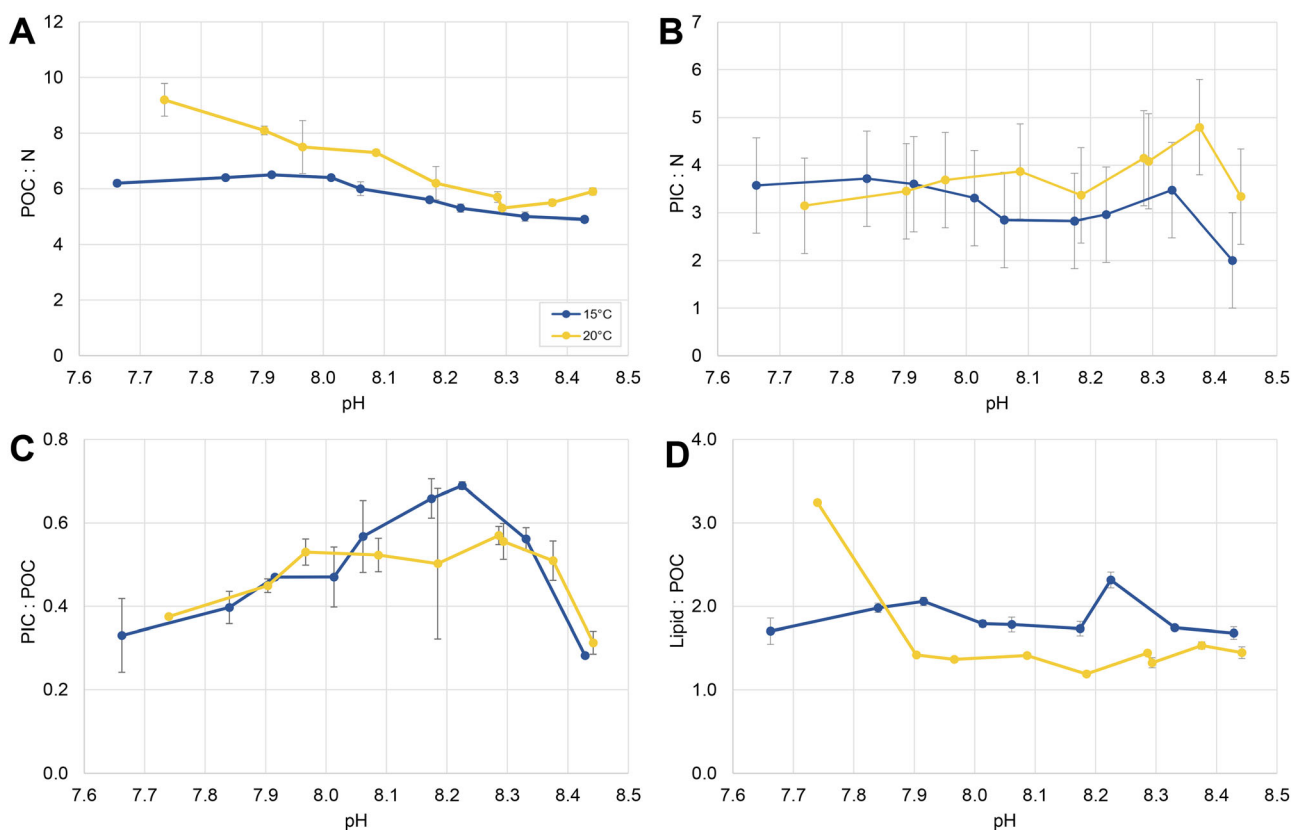


Fig. 4. Carbon ratios in response to pH levels and temperatures. **(A)** POC : nitrogen ratio (POC : N), **(B)** PIC : nitrogen ratio (PIC : N), **(C)** PIC : POC, and **(D)** cellular lipid quota : cellular particulate organic carbon quota (lipid : POC). Error bars indicate data standard deviation within each treatment, not between replicates.

Cellular PIC content (pg cell^{-1}) followed a similar parabolic trend at both temperatures (Fig. 2C). Average cellular PIC content at 20°C ($13.48 \text{ pg cell}^{-1}$; $\text{SD} = 4.95$) was slightly higher than at 15°C ($12.22 \text{ pg cell}^{-1}$; $\text{SD} = 4.38$), both similar to the overall average of $12.85 \text{ pg cell}^{-1}$ ($\text{SD} = 4.58$). The highest cellular PIC content was $21.34 \text{ pg cell}^{-1}$ at 20°C and pH 7.97 (Fig. 2C). PIC content responded in a cubic relationship with pH, which was the only significant predictor (Supporting Information Table S2). Temperature and the interaction between temperature and pH are still included in the model (lowest AIC score).

Cellular Chl *a* content followed distinctly different trends at 15°C and 20°C and was stable across the pH range at 15°C, while 20°C exhibited a clear negative trend from low to high pH (Fig. 2D). Average cellular Chl *a* content at 15°C was $0.27 \text{ pg cell}^{-1}$ ($\text{SD} = 0.03$) and $0.44 \text{ pg cell}^{-1}$ ($\text{SD} = 0.18$) at 20°C. A linear term for pH was significant in the selected model. Temperature, pH, and their interaction were significant predictors for cellular Chl *a* content (Supporting Information Table S2).

Production rates

The average growth rate (day^{-1}) over both temperatures was $0.74 \text{ (day}^{-1}\text{; SD} = 0.13)$ with a range of $0.55\text{--}0.98 \text{ (day}^{-1}\text{)}$.

The growth rate at 20°C was distinctly higher with an average rate of $0.86 \text{ (day}^{-1}\text{; SD} = 0.07\text{; range} = 0.75\text{--}0.98)$ compared with $0.62 \text{ (day}^{-1}\text{; SD} = 0.04\text{; range} = 0.55\text{--}0.67)$ at 15°C. Growth rate showed no clear trend from low to high pH (Fig. 3A). The growth rate at 20°C was overall higher than at 15°C, with a visible trend of decreasing growth rate with decreasing pH. Temperature, pH (quadratic), and the interaction between temperature and pH were significant predictors of the growth rate response for *E. huxleyi* (Supporting Information Table S2).

The average lipid production for both temperatures was $32.68 \text{ pg cell}^{-1} \text{ d}^{-1}$ ($\text{SD} = 6.95\text{; range} = 20.19\text{--}46.31 \text{ pg cell}^{-1} \text{ d}^{-1}$), with each temperature group having similar average values (15°C = 29.86 and 20°C = $35.49 \text{ pg cell}^{-1} \text{ d}^{-1}$; Supporting Information Table S2). Lipid production increased as pH decreased; however, this response varied between temperatures, particularly at the lower range of pH (Fig. 3B). Temperature and pH (quadratic) were significant predictors for lipid production in *E. huxleyi* (Supporting Information Table S2).

The average POC production at 20°C ($23.62 \text{ pg cell}^{-1} \text{ d}^{-1}$; $\text{SD} = 6.34$) was higher than at 15°C ($16.01 \text{ pg cell}^{-1} \text{ d}^{-1}$; $\text{SD} = 2.44$). There was a bell curve trend at 20°C, with a higher

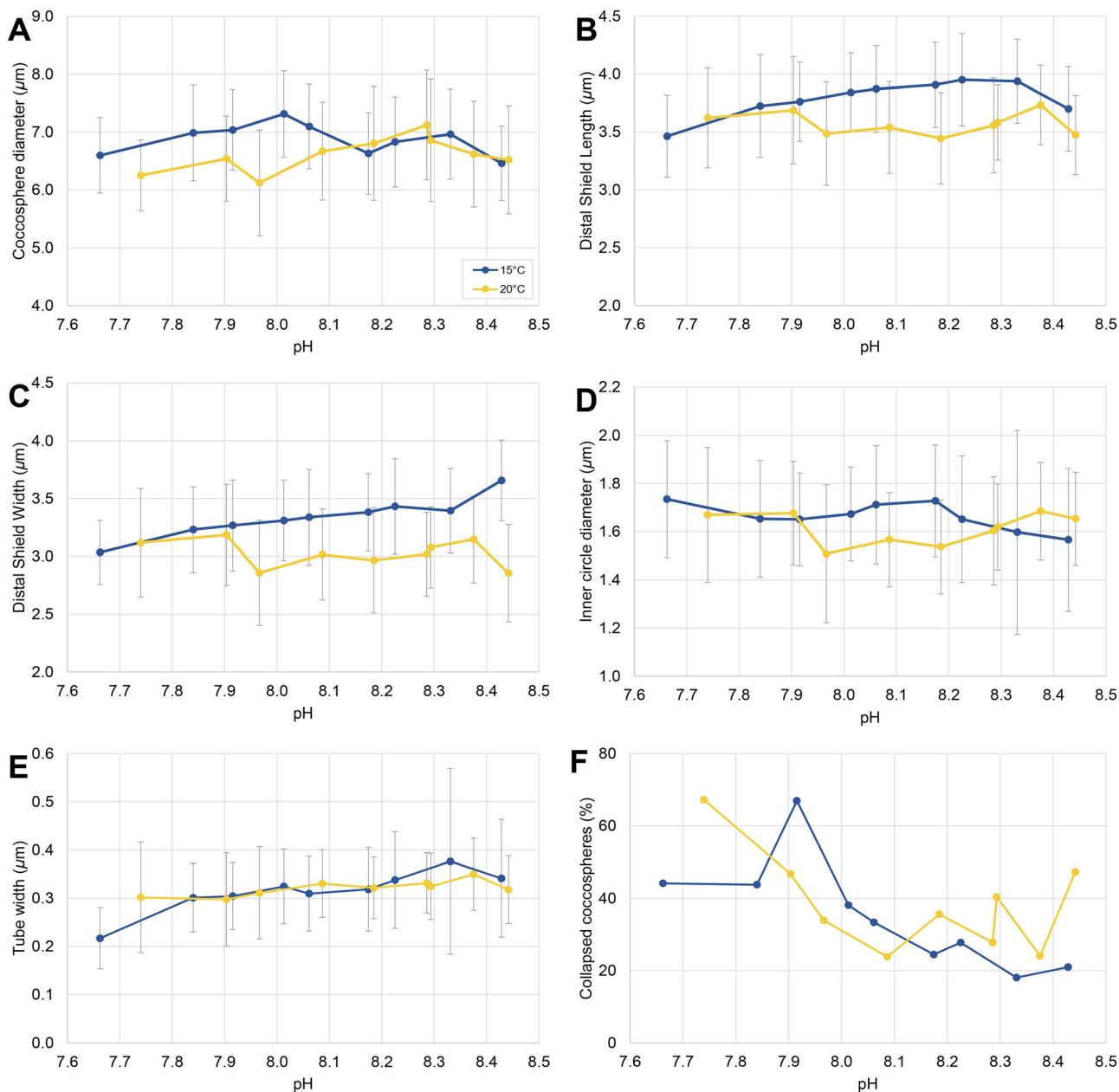


Fig. 5. Coccospere morphological characteristics in response to pH levels and temperatures. **(A)** Coccospere diameter (μm), **(B)** distal shield length (μm), **(C)** distal shield width (μm), **(D)** inner circle diameter (μm), **(E)** tube width (μm), and **(F)** collapsed coccospores (%). Error bars indicate data standard deviation within each treatment, not between replicates (not applicable for collapsed coccospores as percentage was calculated from a single filter).

POC production within the middle of the pH range, while there was no clear trend at 15°C (Fig. 3C). The selected model included a significant quadratic term for pH, which was the only significant predictor of POC production for *E. huxleyi* (Supporting Information Table S2).

The average PIC production ($\text{pg cell}^{-1} \text{d}^{-1}$) was higher at 20°C ($11.57 \text{ pg cell}^{-1} \text{d}^{-1}$; $\text{SD} = 4.29$) than at 15°C ($7.71 \text{ pg cell}^{-1} \text{d}^{-1}$; $\text{SD} = 2.94$), with a bell curve trend across the pH range, which was more pronounced at the higher temperature

(Fig. 3D). The selected model included a significant cubic term for pH, and temperature and pH were both significant predictors for POC production (Supporting Information Table S2).

Chl *a* production ($\text{pg cell}^{-1} \text{d}^{-1}$) remained stable across all pH levels at 15°C (average = $0.15 \text{ pg cell}^{-1}$; $\text{SD} = 0.04$), while it gradually declined from low to high pH at 20°C (average = $0.32 \text{ pg cell}^{-1}$; $\text{SD} = 0.15$; Fig. 3E). Temperature and pH (quadratic) were significant predictors for Chl *a* production (Supporting Information Table S2).

The production potential of lipids showed a clear difference between 15°C and 20°C, and there was a trend of increasing production potential as pH increased, but only at 20°C (Fig. 3F). This largely followed the pattern of growth rate (Fig. 3A), showing that growth rate was the major factor driving the production potential for *E. huxleyi* here. Similar to growth rate, the quadratic term for pH was significant in the selected model. Temperature, pH, and their interaction were significant predictors of the production potential of lipids (Supporting Information Table S2).

Carbon ratios

Mean POC : N ratio for all treatments was 6.28 (range 4.9–9.2). POC : N ratios were higher at 20°C (6.74; SD = 1.35) than at 15°C (6.74; SD = 1.35). Both temperatures followed a similar trend of decreasing POC : N with increasing pH (Fig. 4A). This trend was stronger at 20°C. The cubic term for pH was significant in the selected model, and pH, temperature, and their interaction were significant predictors of the POC : N response in *E. huxleyi* (Supporting Information Table S2).

Similar to POC : N, PIC : N ratios were higher at 20°C (\bar{x} = 3.77; SD = 0.52) than at 15°C (\bar{x} = 3.15; SD = 0.55); however, this difference was not as distinct. At low pH, PIC : N showed similar values for both temperatures; however, at approximately pH 8.0 and above, the response curves started to diverge, with PIC : N values higher at 20°C than at 15°C (Fig. 4B). Temperature and the interaction between temperature and pH were significant predictors of the PIC : N response of *E. huxleyi* (Supporting Information Table S2). For PIC : N, pH is still included in the selected model and was minorly significant ($p < 0.1$).

The average PIC : POC ratio was similar across both temperatures (15°C = 0.49, SD = 0.14; 20°C = 0.48, SD = 0.09); however, PIC : POC had a parabolic relationship with pH, with the highest ratios in the middle range of the pH range, where it reached a maximum of 0.69 at pH 8.23 before declining toward low and high pH (Fig. 4C). Both temperatures followed this relationship curve, and the results of the GLM indicate that pH (cubic term) was a significant predictor of the PIC : POC response of *E. huxleyi* (Supporting Information Table S2).

The lipid : POC ratio overall was higher at 15°C (average = 1.87, SD = 0.21) than at 20°C (average = 1.6, SD = 0.63), except at pH 7.74, where the ratio distinctly increases at 20°C (Fig. 4D). Temperature was a significant predictor for lipid : POC (Supporting Information Table S2).

Morphology

Coccosphere diameter (μm) followed similar trends for both temperatures in the higher pH range; however, at low pH, coccosphere diameter was smaller at 20°C (Fig. 5A). The selected model includes a significant quadratic term for pH and temperature, and their interaction was significant

predictors of coccosphere diameter for *E. huxleyi* (Supporting Information Table S2).

Distal shield length (μm) was greater at 15°C than 20°C. It also exhibited slight bell curve response at 15°C (Fig. 5B). A quadratic term for pH was significant in the selected model and temperature and pH were significant predictors for distal shield length (Supporting Information Table S2). Distal shield width (μm) followed a similar pattern to distal shield length; however, here only temperature and the interaction between temperature and pH were significant predictors (Fig. 5C; Supporting Information Table S2). Although pH was a nonsignificant term for the model, it was retained as it is included in the interaction. It may be the effect of high variability associated with distal shield length that may explain why pH was not a significant predictor here.

Average inner circle diameter (μm) remained largely stable across pH at both temperatures, however, was highly variable. Inner circle diameter had no significant predictors (Fig. 5D; Supporting Information Table S2). Coccolith tube width increased with increasing pH for both temperatures, and pH was a significant predictor (Fig. 5E; Supporting Information Table S2).

Overall, collapsed coccospheres (%) made up approximately 37% of the cells. This differed with temperature, with an average of 35% at 15°C, and 39% at 20°C. A cubic term for pH was significant in the selected model and is the only significant predictor for collapsed coccospheres (Supporting Information Table S2), with the percentage of collapsed coccospheres increasing toward the lower pH range (Fig. 5F). Temperature and the interaction between temperature and pH were not significant; however, they were included in the selected model (lowest AIC score).

Discussion

Consumer impacts

Food quantity

In this study, we show that temperature is an important predictor for the production potential of lipids, indicating increases in lipid availability under ocean warming. This increase will likely be energetically favorable for consumers. pH is also a significant predictor of the production potential of lipids, and the results suggest that this increase in availability will be mitigated by ocean acidification. The availability of lipids in coccolithophores for their consumers is important when investigating potential energy transfer between trophic levels and to understand how this may change under ocean acidification and warming. The production potential of lipids is strongly influenced by the growth rate, and it is distinctly higher under the warmer temperature (Fig. 3F). The decrease in production potential under low pH was mostly related to the impact of pH on growth rate, rather than the impact of pH on cellular lipid quota, which increased under lower pH (Fig. 2A). At any rate, this suggests that consumers may be

positively affected by the increased quantity of available cells, and in warmer conditions, there will be greater lipid availability, which is likely to be energetically beneficial for coccolithophore consumers.

Food quality

The interaction between pH and temperature was an important driver for POC : N which was higher at low pH (~ 7.9 – 7.7) and 20°C (Fig. 4A), indicating that the availability of nitrogen for coccolithophore consumers will be reduced under ocean acidification and warming. Nitrogen is essential for cellular function and is involved in the production of macromolecules, such as proteins or amino acids, including chlorophyll (Riegman et al. 2000). A higher POC : N suggests a lower quality food as a higher ratio of carbon can indicate nitrogen limitation. The mean POC : N ratio across all treatments is similar to the Redfield ratio of 6.3 (Martiny et al. 2014); however, this average differs with temperature. The range of POC : N is similar to what is expected in natural populations of phytoplankton (Geider and La Roche 2002) and experimental work with coccolithophores (Fiorini et al. 2010). Contrary to our results, there was no significant effect of elevated $p\text{CO}_2$ ($760 \mu\text{atm}$ corresponding to pH 7.81) on POC : N for *E. huxleyi* strain (AC472) from the South Pacific (Fiorini et al. 2010). However, the difference in pH levels was not as pronounced as they are in this experiment. For instance, an increase in POC : N was also reported under elevated $p\text{CO}_2$ for *E. huxleyi* using a wider range of pH levels (6.8–8.3; Iglesias-Rodriguez et al. 2008—morphotype R). Under ocean acidification conditions, the reduced nitrogen availability might have negative impacts on micrograzers that have issues with nitrogen limitation.

Lipid content is also an important indicator of the nutritional quality of coccolithophores for secondary consumers (Pond and Harris 1996), as also seen for diatoms in particular, and plankton in general (Rossoll et al. 2012; Meyers et al. 2019). Although we see greater availability of *E. huxleyi* in terms of the production potential of lipids (Fig. 3F), given that the availability of nitrogen under both ocean acidification and warming will be reduced (Fig. 4A), the quality of coccolithophores as a food source will likely be negatively impacted (Conde-Porcuna et al. 2002; Mitra and Flynn 2005; Iglesias-Rodriguez et al. 2008). However, as cellular lipid content is predicted to either be unaffected (Fiorini et al. 2010) or increase under ocean acidification conditions, as is the case here (Fig. 2A), the nutritional impacts on coccolithophore consumers will likely be varied. From the perspective of lipid : POC, however, food quality appears unaltered (Kharbush et al. 2020) except under the lowest pH at 20°C , which is exceptionally high (Fig. 4D). This increase might indicate a crossed threshold under ocean acidification conditions at 20°C involving a carbon storage strategy related to extreme stress which has been previously reported for both

microalgae and macroalgae (Kuwata et al. 1993; Fuentes-Grünewald et al. 2012; Prabhu et al. 2019).

Coccosphere integrity and PIC : POC Ratio

Coccoliths can diminish the nutritional value of coccolithophores in three ways. First, through mechanical protection, making it more difficult for grazers to access the protoplast (Haunost et al. 2021). Second, through the need to counteract the increase in the pH of guts or food vacuoles due to carbonate dissolution (Harvey et al. 2015). Third, through reduction in the percentage of digestible material (Haunost et al. 2021). While the first point hinges on morphology, the last two points center on the amount of calcite relative to organic material. To assess the first point, we focus on the percentage of collapsed coccospheres, which indicates reduced mechanical stability (Jaya et al. 2016), and to assess the last two points, we analyzed the PIC : POC ratio.

The percentage of collapsed coccospheres increased with decreasing pH at both temperatures, indicating reduced structural integrity of the coccosphere (Fig. 5F). Copepods do not need to destroy the coccosphere as they have to in the case of the diatom frustule (Langer et al. 2007; Jansen 2008); however, dinoflagellates need to penetrate the coccosphere to digest the cell contents, and then egest the remaining indigestible calcium carbonate (Haunost et al. 2021). This means that if the interlocking between coccoliths is reduced, dinoflagellates may be able to more readily access coccolithophore cell contents, potentially aiding in digestion.

The PIC : POC ratio was unaffected by temperature; however, we observed a distinct bell-curve in response to pH under both temperatures (Fig. 2H). Although PIC : POC response patterns are strain specific (Langer et al. 2009; Rosas-Navarro et al. 2016), a meta-analysis suggests a negative correlation between PIC : POC and pH (Meyer and Riebesell 2015). Taken together, the PIC : POC ratio and the coccosphere integrity response suggest that ocean acidification will make it easier for grazers to digest coccolithophores and access cell contents. Therefore, macrograzers such as copepods will likely benefit from the higher percentage of digestible material, and less so from both the reduced structural integrity of the coccosphere and the potentially negligible gut pH change (Harris 1994; Nejstgaard et al. 1997; Langer et al. 2007b; White et al. 2018; Mayers et al. 2020). Micrograzers such as dinoflagellates will likely benefit from all three aspects of coccolith-related nutritional value change (Harvey et al. 2015; Jaya et al. 2016; Haunost et al. 2021).

Individual response

Physiological rates

The response to ocean acidification conditions in terms of physiological rates generally shows high inter- and intra-species variability (Langer et al. 2009; Hoppe et al. 2011). After initial uncertainty as to the interpretation of this variability, the work of Bach and co-authors has produced a plausible and

now widely accepted interpretation using substrate–inhibitor concept (Bach et al. 2011, 2013, 2015; Paul and Bach 2020), which states that with increasing substrate (CO_2) concentration, POC production increases up to the point when the inhibitory effect of increasing H^+ concentration then causes a decrease in POC production (ca. pH 8 in our data, Fig. 3C). In these studies, it was shown that the response of coccolithophores to seawater carbonate chemistry changes is best thought of as a bell curve, with different strains featuring different optima. In our case, we can see the bell curve in the PIC and POC production, while other rates display only part of the full bell curve (Fig. 4A,B,F,E). Growth rate, for instance, shows a somewhat atypical increase at 20°C (Iglesias-Rodriguez et al. 2008; Langer et al. 2009—morphotypes A, B, R; Mackey et al. 2015); however, the dependence of growth rate on temperature has been seen in several coccolithophorid strains (Buitenhuis et al. 2008; Fielding 2013). The response patterns over the pH range tested here do not appear to be related to morphotype or other easily identifiable strain features (see also Krumhardt et al. 2017).

Morphological parameters as PIC production proxy

The decrease in PIC production does not correlate with changes in any morphological characteristics at both temperatures or across the pH range. Coccosphere size and coccolith weight (usually correlated with coccolith size) have been proposed as proxies for PIC production (Beaufort et al. 2011; Bach et al. 2012; Gibbs et al. 2013). In contrast to our study, Rosas-Navarro et al. (2016) described a positive correlation of coccolith size and PIC production in three *E. huxleyi* strains. This discrepancy could stem from strain specificity but seems unrelated to morphotype because all strains considered here are Morphotype A. A widespread strain specificity in the relationship between coccolith size and PIC production would make the application of this proxy difficult.

Future ramifications

Future coccolithophore consumers will likely benefit from an energetic standpoint, due to the increase in lipid availability under ocean warming; however, this increase will be mitigated by ocean acidification. As this experiment was done under nutrient replete exponential growth, concurrent changes in nutrient availability may alter these impacts on the nutritional condition of *E. huxleyi* (Müller et al. 2017). From a functional point of view, a higher POC : N will not contribute as much to cell function for consumers, and as such, the capacity of coccolithophores to provide a healthy food source may be reduced. The nutritional quality of coccolithophores as indicated by POC : N, lipid : POC, and PIC : POC will likely have varied impacts, depending on an organism's specific requirements. For example, organisms with limited nutrient supplies could be affected by increases in POC : N under future conditions, while organisms that have

difficulty digesting calcite may benefit from decreases in PIC : POC under ocean acidification.

Phytoplankton biomass is predicted to have a varied response to ocean acidification and warming, and this response will largely vary depending on latitude and taxonomic group (Seifert et al. 2020). Due to the calcifying nature of coccolithophores, they will have the additional stress of reduced seawater pH (Guinder and Molinero 2013), affecting their ability to calcify (Riebesell et al. 2000; Engel et al. 2005; Hoppe et al. 2011; Lefebvre et al. 2011; Schlüter et al. 2014) and potentially pushing them closer to a stress response than noncalcifying plankton. Although adaptation to ocean acidification and warming has been shown to occur relatively rapidly in *E. huxleyi* (1 yr for PIC and POC to return to present-day levels; growth 16% higher than nonadapted controls after 1 yr; Schlüter et al. 2014), for the coccolithophore *Gephyrocapsa oceanica*, growth rate (after an initial increase), POC production, and nitrogen production all decreased over 2000 generations (approximately 1400 d) under high CO_2 conditions, indicating that resilience to ocean acidification conditions can reduce over time (Jin and Gao 2016). In another experiment, *E. huxleyi* cells adjusted their chlorophyll content more rapidly than other coccolithophore species (Lewis et al. 1984), potentially as an adaptive photosynthetic trait to changing ocean conditions (Feng et al. 2008). This suggests that the ability to adapt to ocean acidification conditions will likely vary depending on the species and physiological parameter in question.

We may see future shifts in *E. huxleyi* ranges as they shift to warmer areas where they achieve a more favorable growth rate (Neukermans et al. 2018), and this may further affect other organisms that rely on coccolithophores as a food source. Despite inter- and intra-species variability in response patterns (Langer et al. 2006, 2009), our results suggest that combined low pH and an increased temperature has the potential to increase coccolithophore lipid standing stock, but decrease food quality, as inferred from an increased POC : N ratio.

The short-term experiment presented here provides us with important information about the immediate response of coccolithophores to changes in temperature and pH, and this can be decisive in field scenarios, particularly in cases where populations are not given the opportunity to adapt. Further work investigating the long-term impact of ocean acidification and warming on the nutritional content (in terms of both quality and quantity) of coccolithophores, a globally important phytoplankton at the base of the marine food web, will be a key part of understanding the impacts of climate change on ocean trophic dynamics.

Data availability statement

The data that support the findings of this study will be available from PANGAEA.de and are also available from the corresponding author, R.J., upon request.

References

- Aho, K., D. Derryberry, and T. Peterson. 2014. Model selection for ecologists: The worldviews of AIC and BIC. *Ecology* **95**: 631–636. doi:10.1890/13-1452.1
- Arnold, H. E., P. Kerrison, and M. Steinke. 2013. Interacting effects of ocean acidification and warming on growth and DMS-production in the haptophyte coccolithophore *Emiliania huxleyi*. *Global Chang. Biol.* **19**: 1007–1016. doi:10.1111/gcb.12105
- Bach, L. T., U. Riebesell, and K. G. Schulz. 2011. Distinguishing between the effects of ocean acidification and ocean carbonation in the coccolithophore *Emiliania huxleyi*. *Limnol. Oceanogr.* **56**: 2040–2050. doi:10.4319/lo.2011.56.6.2040
- Bach, L. T., C. Bauke, K. J. S. Meier, U. Riebesell, and K. G. Schulz. 2012. Influence of changing carbonate chemistry on morphology and weight of coccoliths formed by *Emiliania huxleyi*. *Biogeosciences* **9**: 3449–3463. doi:10.5194/bg-9-3449-2012
- Bach, L. T., L. C. M. Mackinder, K. G. Schulz, G. Wheeler, D. C. Schroeder, C. Brownlee, and U. Riebesell. 2013. Dissecting the impact of CO₂ and pH on the mechanisms of photosynthesis and calcification in the coccolithophore *Emiliania huxleyi*. *New Phytol.* **199**: 121–134. doi:10.1111/nph.12225
- Bach, L. T., U. Riebesell, M. A. Gutowska, L. Federwisch, and K. G. Schulz. 2015. A unifying concept of coccolithophore sensitivity to changing carbonate chemistry embedded in an ecological framework. *Prog. Oceanogr.* **135**: 125–138. doi:10.1016/j.pocean.2015.04.012
- Barnes, H., and J. Blackstock. 1973. Estimation of lipids in marine animals and tissues: Detailed investigation of the sulphophosphovanilun method for 'total' lipids. *J. Exp. Mar. Bio. Ecol.* **12**: 103–118. doi:10.1016/0022-0981(73)90040-3
- Beaufort, L., and others. 2011. Sensitivity of coccolithophores to carbonate chemistry and ocean acidification. *Nature* **476**: 80–83. doi:10.1038/nature10295, 7358
- Bendle, J., A. Rosell-Melé, and P. Ziveri. 2005. Variability of unusual distributions of alkenones in the surface waters of the Nordic seas. *Paleoceanography* **20**. doi:10.1029/2004PA001025
- Breteler, W. C. M., N. Schogt, and S. Rampen. 2005. Effect of diatom nutrient limitation on copepod development: Role of essential lipids. *Mar. Ecol. Prog. Ser.* **291**: 125–133. doi:10.3354/meps291125
- Broglio, E., S. Jonasdottir, A. Calbet, H. Jakobsen, and E. Saiz. 2003. Effect of heterotrophic versus autotrophic food on feeding and reproduction of the calanoid copepod *Acartia tonsa*: Relationship with prey fatty acid composition. *Aquat. Microb. Ecol.* **31**: 267–278.
- Brown, C. W., and J. A. Yoder. 1994. Coccolithophorid blooms in the global ocean. *J. Geophys. Res. Ocean* **99**: 7467–7482. doi:10.1029/93JC02156
- Buitenhuis, E. T., P. T. D. J. Franklin, and others. 2008. Growth rates of six coccolithophorid strains as a function of temperature. *Limnol. Oceanogr.* **53**: 1181–1185. doi:10.4319/lo.2008.53.3.1181
- Chavez, F. P., M. Messié, and J. T. Pennington. 2010. Marine primary production in relation to climate variability and change. *Ann. Rev. Mar. Sci.* **3**: 227–260. doi:10.1146/annurev.marine.010908.163917
- Conde-Porcuna, J. M., E. Ramos-Rodriguez, and C. Perez-Martinez. 2002. Correlations between nutrient concentrations and zooplankton populations in a mesotrophic reservoir. *Freshw. Biol.* **47**: 1463–1473. doi:10.1046/j.1365-2427.2002.00882.x
- Cottingham, K. L., J. T. Lennon, and B. L. Brown. 2005. Knowing when to draw the line: Designing more informative ecological experiments. *Front. Ecol. Environ.* **3**: 145–152. doi:10.1890/1540-9295(2005)003[0145:KWTDTL]2.0.CO;2.
- Cripps, G., K. J. J. Flynn, and P. K. K. Lindeque. 2016. Ocean acidification affects the phyto-zoo plankton trophic transfer efficiency. *PLoS One* **11**: e0151739.
- D'Amario, B., P. Ziveri, M. Grelaud, A. Oviedo, and M. Kralj. 2017. Coccolithophore haploid and diploid distribution patterns in the Mediterranean Sea: Can a haplo-diploid life cycle be advantageous under climate change? *J. Plankton Res.* **39**: 781–794. doi:10.1093/plankt/fbx044
- Doney, S. C., V. J. Fabry, R. A. Feely, and J. A. Kleypas. 2009. Ocean acidification: The other CO₂ problem. *Ann. Rev. Mar. Sci.* **1**: 169–192. doi:10.1146/annurev.marine.010908.163834
- El-Hady, H., S. Fathey, G. Ali, and Y. Gabr. 2016. Biochemical profile of phytoplankton and its nutritional aspects in some khors of Lake Nasser, Egypt. *Egypt. J. Basic Appl. Sci.* **3**: 187–193. doi:10.1016/j.ejbas.2016.03.002
- Engel, A., and others. 2005. Testing the direct effect of CO₂ concentration on a bloom of the coccolithophorid *Emiliania huxleyi* in mesocosm experiments. *Limnol. Oceanogr.* **50**: 493–507. doi:10.4319/lo.2005.50.2.0493
- Fabry, V. J., B. A. Seibel, R. A. Feely, and J. C. Orr. 2008. Impacts of ocean acidification on marine fauna and ecosystem processes. *ICES J. Mar. Sci.* **65**: 414–432. doi:10.1093/icesjms/fsn048
- Falkowski, P. G., T. Fenchel, and E. F. Delong. 2008. The microbial engines that drive earth's biogeochemical cycles. *Science* **320**: 1034–1039. doi:10.1126/science.1153213
- Feng, Y., M. E. Warner, Y. Zhan, J. Sun, F. Fu, J. M. Rose, and D. A. Hutchins. 2008. Interactive effects of increased pCO₂, temperature and irradiance on the marine coccolithophore *Emiliania huxleyi* (Prymnesiophyceae). *Eur. J. Phycol.* **43**: 87–98. doi:10.1080/09670260701664674
- Feng, Y., M. Y. Roleda, E. Armstrong, P. W. Boyd, and C. L. Hurd. 2017. Environmental controls on the growth, photosynthetic and calcification rates of a Southern Hemisphere strain of the coccolithophore *Emiliania huxleyi*. *Limnol. Oceanogr.* **62**: 519–540. doi:10.1002/lno.10442

- Fielding, S. R. R. 2013. *Emiliania huxleyi* specific growth rate dependence on temperature. *Limnol. Oceanogr.* **58**: 663–666. doi:10.4319/lo.2013.58.2.0663
- Fiorini, S., J.-P. Gattuso, P. van Rijswijk, and J. J. Middelburg. 2010. Coccolithophores lipid and carbon isotope composition and their variability related to changes in seawater carbonate chemistry. *J. Exp. Mar. Biol. Ecol.* **394**: 74–85. doi:10.1016/j.jembe.2010.07.020
- Fraser, A. J., J. R. Sargent, J. C. Gamble, and D. D. Seaton. 1989. Formation and transfer of fatty acids in an enclosed marine food chain comprising phytoplankton, zooplankton and herring (*Clupea harengus* L.) larvae. *Mar. Chem.* **27**: 1–18. doi:10.1016/0304-4203(89)90024-8
- Fuentes-Grünwald, C., E. Garcés, E. Alacid, N. Sampedro, S. Rossi, and J. Camp. 2012. Improvement of lipid production in the marine strains *Alexandrium minutum* and *Heterosigma akashiwo* by utilizing abiotic parameters. *J. Ind. Microbiol. Biotechnol.* **39**: 207–216. doi:10.1007/s10295-011-1016-6
- Fukuda, S. Y., Y. Suzuki, and Y. Shiraiwa. 2014. Difference in physiological responses of growth, photosynthesis and calcification of the coccolithophore *Emiliania huxleyi* to acidification by acid and CO₂ enrichment. *Photosynth. Res.* **121**: 299–309. doi:10.1007/s11120-014-9976-9
- Gafar, N. A., B. D. Eyre, and K. G. Schulz. 2018. A conceptual model for projecting coccolithophorid growth, calcification and photosynthetic carbon fixation rates in response to global ocean change. *Front. Mar. Sci.* **4**: 433.
- Geider, R., and J. La Roche. 2002. Redfield revisited: Variability of C:N:P in marine microalgae and its biochemical basis. *Eur. J. Phycol.* **37**: 1–17. doi:10.1017/S0967026201003456
- Gibbs, S. J., and others. 2013. Species-specific growth response of coccolithophores to Palaeocene–Eocene environmental change. *Nat. Geosci.* **6**: 218–222. doi:10.1038/ngeo1719
- Gili, J.-M., and R. Coma. 1998. Benthic suspension feeders: Their paramount role in littoral marine food webs. *Trends Ecol. Evol.* **13**: 316–321. doi:10.1016/S0169-5347(98)01365-2
- Gori, A., and others. 2013. Effects of food availability on the sexual reproduction and biochemical composition of the Mediterranean gorgonian *Paramuricea clavata*. *J. Exp. Mar. Biol. Ecol.* **444**: 38–45. doi:10.1016/j.jembe.2013.03.009
- Guinder, V., and J. Molinero. 2013. Climate change effects on marine phytoplankton, p. 68–90. *In* Marine ecology in a changing world. CRC Press.
- Harris, R. P. 1994. Zooplankton grazing on the coccolithophore *Emiliania huxleyi* and its role in inorganic carbon flux. *Mar. Biol.* **119**: 431–439. doi:10.1007/BF00347540
- Harvey, E. L., K. D. Bidle, and M. D. Johnson. 2015. Consequences of strain variability and calcification in *Emiliania huxleyi* on microzooplankton grazing. *J. Plankton Res.* **37**: 1137–1148. doi:10.1093/plankt/fbv081
- Haunost, M., U. Riebesell, F. D'Amore, O. Kelting, and L. T. T. Bach. 2021. Influence of the calcium carbonate shell of coccolithophores on ingestion and growth of a dinoflagellate predator. *Front. Mar. Sci.* **8**.
- Holligan, P. M., and others. 1993. A biogeochemical study of the coccolithophore, *Emiliania huxleyi*, in the North Atlantic. *Global Biogeochem. Cycl.* **7**: 879–900. doi:10.1029/93GB01731
- Hoppe, C. J. M., G. Langer, and B. Rost. 2011. *Emiliania huxleyi* shows identical responses to elevated pCO₂ in TA and DIC manipulations. *J. Exp. Mar. Biol. Ecol.* **406**: 54–62. doi:10.1016/j.jembe.2011.06.008
- Iglesias-Rodriguez, M. D., and others. 2008. Phytoplankton calcification in a high-CO₂ world. *Science* **320**: 336–340. doi:10.1126/science.1154122
- IPCC. 2019. IPCC special report on the ocean and cryosphere in a changing climate. IPCC.
- Jansen, S. 2008. Copepods grazing on *Coscinodiscus wailesii*: A question of size? *Helgoland Mar. Res.* **62**: 251–255. doi:10.1007/s10152-008-0113-z
- Jaya, B. N., R. Hoffmann, C. Kirchlechner, G. Dehm, C. Scheu, and G. Langer. 2016. Cocospheres confer mechanical protection: New evidence for an old hypothesis. *Acta Biomater.* **42**: 258–264. doi:10.1016/j.actbio.2016.07.036
- Jeffrey, S. W., and G. F. Humphrey. 1975. New spectrophotometric equations for determining chlorophylls a, b, c1 and c2 in higher plants, algae and natural phytoplankton. *Biochem. Physiol. Pflanz.* **167**: 191–194. doi:10.1016/S0015-3796(17)30778-3
- Jin, P., and K. Gao. 2016. Reduced resilience of a globally distributed coccolithophore to ocean acidification: Confirmed up to 2000 generations. *Mar. Pollut. Bull.* **103**: 101–108. doi:10.1016/j.marpolbul.2015.12.039
- Jin, P., D. A. A. Hutchins, and K. Gao. 2020. The impacts of ocean acidification on marine food quality and its potential food chain consequences. *Front. Mar. Sci.* **7**.
- Keller, M. D., R. C. Selvin, W. Claus, and R. R. L. Guillard. 1987. Media for the culture of oceanic ultraphytoplankton. *J. Phycol.* **23**: 633–638. doi:10.1111/j.1529-8817.1987.tb04217.x
- Kharbush, J. J., and others. 2020. Particulate organic carbon deconstructed: Molecular and chemical composition of particulate organic carbon in the ocean. *Front. Mar. Sci.* **7**: 518.
- Klaas, C., and D. E. Archer. 2002. Association of sinking organic matter with various types of mineral ballast in the deep sea: Implications for the rain ratio. *Global Biogeochem. Cycl.* **16**: 63–163–14. doi:10.1029/2001GB001765
- Klauschie, T., B. Bauer, N. Aberle-Malzahn, U. Sommer, and U. Gaedke. 2012. Climate change effects on phytoplankton depend on cell size and food web structure. *Mar. Biol.* **159**: 2455–2478. doi:10.1007/s00227-012-1904-y
- Klitzsch, T., G. Langer, G. Nehrke, A. Wieland, K. Lenhart, and F. Keppler. 2019. Methane production by three widespread marine phytoplankton species: Release rates,

- precursor compounds, and potential relevance for the environment. *Biogeosciences* **16**: 4129–4144. doi:[10.5194/bg-16-4129-2019](https://doi.org/10.5194/bg-16-4129-2019)
- Kottmeier, D. M., A. Chrachri, G. Langer, K. E. Helliwell, G. L. Wheeler, and C. Brownlee. 2022. Reduced H⁺ channel activity disrupts pH homeostasis and calcification in coccolithophores at low ocean pH. *Proc. Natl. Acad. Sci.* **119**: e2118009119. doi:[10.1073/pnas.2118009119](https://doi.org/10.1073/pnas.2118009119)
- Krumhardt, K. M., N. S. Lovenduski, M. D. Iglesias-Rodriguez, and J. A. Kleypas. 2017. Coccolithophore growth and calcification in a changing ocean. *Prog. Oceanogr.* **159**: 276–295. doi:[10.1016/j.pocean.2017.10.007](https://doi.org/10.1016/j.pocean.2017.10.007)
- Kuwata, A., T. Hama, and M. Takahashi. 1993. Ecophysiological characterization of two life forms, resting spores and resting cells, of a marine planktonic diatom, *Chaetoceros pseudocunisetus*, formed under nutrient depletion. *Mar. Ecol. Prog. Ser.* **102**: 245–255. doi:[10.3354/meps102245](https://doi.org/10.3354/meps102245)
- Langer, G., M. Geisen, K. H. Baumann, J. Klas, U. Riebesell, S. Thoms, and J. R. Young. 2006. Species-specific responses of calcifying algae to changing seawater carbonate chemistry. *Geochem. Geophys. Geosyst.* **7**: Q09006. doi:[10.1029/2005GC001227](https://doi.org/10.1029/2005GC001227)
- Langer, G., G. Nehrke, and S. Jansen. 2007. Dissolution of *Calcidiscus leptoporus* coccoliths in copepod guts? A morphological study. *Mar. Ecol. Prog. Ser.* **331**: 139–146. doi:[10.3354/meps331139](https://doi.org/10.3354/meps331139)
- Langer, G., G. Nehrke, I. Probert, J. Ly, and P. Ziveri. 2009. Strain-specific responses of *Emiliania huxleyi* to changing seawater carbonate chemistry. *Biogeosciences* **6**: 2637–2646. doi:[10.5194/bg-6-2637-2009](https://doi.org/10.5194/bg-6-2637-2009)
- Lefebvre, S. C., and others. 2011. Nitrogen source and pCO₂ synergistically affect carbon allocation, growth and morphology of the coccolithophore *Emiliania huxleyi*: Potential implications of ocean acidification for the carbon cycle. *Glob. Chang. Biol.* **18**: 493–503. doi:[10.1111/j.1365-2486.2011.02575.x](https://doi.org/10.1111/j.1365-2486.2011.02575.x)
- Lewis, M. R., J. J. Cullen, and T. Platt. 1984. Relationships between vertical mixing and photoadaptation of phytoplankton: Similarity criteria. *Mar. Ecol. Prog. Ser.* **15**: 141–149. doi:[10.3354/meps015141](https://doi.org/10.3354/meps015141)
- Litzow, M. 2006. Climate regime shifts and community reorganization in the Gulf of Alaska: How do recent shifts compare with 1976/1977? *ICES J. Mar. Sci.* **63**: 1386–1396. doi:[10.1016/j.icesjms.2006.06.003](https://doi.org/10.1016/j.icesjms.2006.06.003)
- Liu, X., M. C. Patsavas, and R. H. Byrne. 2011. Purification and characterization of meta-cresol purple for spectrophotometric seawater pH measurements. *Environ. Sci. Technol.* **45**: 4862–4868. doi:[10.1021/es200665d](https://doi.org/10.1021/es200665d)
- Mackey, K. R. M., J. J. Morris, F. M. M. Morel, and S. A. Kranz. 2015. Response of photosynthesis to ocean acidification. *Oceanography* **28**: 74–91. doi:[10.5670/oceanog.2015.33](https://doi.org/10.5670/oceanog.2015.33)
- Malinverno, E., F. G. Prahl, B. N. Popp, and P. Ziveri. 2008. Alkenone abundance and its relationship to the coccolithophore assemblage in Gulf of California surface waters. *Deep Sea Res. Part I Oceanogr. Res. Pap.* **55**: 1118–1130. doi:[10.1016/j.dsr.2008.04.007](https://doi.org/10.1016/j.dsr.2008.04.007)
- Martiny, A. C., J. A. Vrugt, and M. W. Lomas. 2014. Concentrations and ratios of particulate organic carbon, nitrogen, and phosphorus in the global ocean. *Sci. Data* **1**: 140048. doi:[10.1038/sdata.2014.48](https://doi.org/10.1038/sdata.2014.48)
- Mayers, K. M. J., and others. 2020. The possession of coccoliths fails to deter microzooplankton grazers. *Front. Mar. Sci.* **7**.
- Meyer, J., and U. Riebesell. 2015. Reviews and syntheses: Responses of coccolithophores to ocean acidification: A meta-analysis. *Biogeosciences* **12**: 1671–1682. doi:[10.5194/bg-12-1671-2015](https://doi.org/10.5194/bg-12-1671-2015)
- Meyers, M. T., W. P. Cochlan, E. J. Carpenter, and W. J. Kimmerer. 2019. Effect of ocean acidification on the nutritional quality of marine phytoplankton for copepod reproduction. *PLoS One* **14**: e0217047. doi:[10.1371/journal.pone.0217047](https://doi.org/10.1371/journal.pone.0217047)
- Milner, S., G. Langer, M. Grelaud, and P. Ziveri. 2016. Ocean warming modulates the effects of acidification on calcification and sinking. *Limnol. Oceanogr.* **61**: 1322–1336. doi:[10.1002/lno.v61.4](https://doi.org/10.1002/lno.v61.4)
- Mitra, A., and K. J. Flynn. 2005. Predator–prey interactions: Is “ecological stoichiometry” sufficient when good food goes bad? *J. Plankton Res.* **27**: 393–399. doi:[10.1093/plankt/fbi022](https://doi.org/10.1093/plankt/fbi022)
- Monteiro, F. M., and others. 2016. Why marine phytoplankton calcify. *Sci. Adv.* **2**: e1501822. doi:[10.1126/sciadv.1501822](https://doi.org/10.1126/sciadv.1501822)
- Müller, M. N., T. W. Trull, and G. M. Hallegraeff. 2017. Independence of nutrient limitation and carbon dioxide impacts on the Southern Ocean coccolithophore *Emiliania huxleyi*. *ISME J.* **11**: 1777–1787. doi:[10.1038/ismej.2017.53](https://doi.org/10.1038/ismej.2017.53)
- Nejstgaard, J. C., I. Gismervik, and P. T. Solberg. 1997. Feeding and reproduction by *Calanus finmarchicus*, and microzooplankton grazing during mesocosm blooms of diatoms and the coccolithophore *Emiliania huxleyi*. *Mar. Ecol. Prog. Ser.* **147**: 197–217.
- Nelder, J. A., and R. W. M. Wedderburn. 1972. Generalized linear models. *J. Roy. Stat. Soc. Ser. A* **135**: 370–384. doi:[10.2307/2344614](https://doi.org/10.2307/2344614)
- Neukermans, G., L. Oziel, and M. Babin. 2018. Increased intrusion of warming Atlantic water leads to rapid expansion of temperate phytoplankton in the Arctic. *Glob. Chang. Biol.* **24**: 2545–2553. doi:[10.1111/gcb.14075](https://doi.org/10.1111/gcb.14075)
- Paul, A. J., and L. T. Bach. 2020. Universal response pattern of phytoplankton growth rates to increasing CO₂. *New Phytol.* **228**: 1710–1716. doi:[10.1111/nph.16806](https://doi.org/10.1111/nph.16806)
- Pierrot, D., D. Wallace, E. Lewis, R. Wallace, and W. Wallace. 2011. MS Excel Program Developed for CO₂ System Calculations. ORNL Environmental Sciences Division. doi:[10.3334/CDIAC/otg](https://doi.org/10.3334/CDIAC/otg)
- Pond, D. W., and R. P. Harris. 1996. The lipid composition of the Coccolithophore *Emiliania huxleyi* and its possible ecophysiological significance. *J. Mar. Biol. Assoc. UK* **76**: 579–594. doi:[10.1017/S0025315400031295](https://doi.org/10.1017/S0025315400031295)

- Prabhu, M., and others. 2019. Starch from the sea: The green macroalga *Ulva ohnoi* as a potential source for sustainable starch production in the marine biorefinery. *Algal Res.* **37**: 215–227. doi:10.1016/j.algal.2018.11.007
- Riebesell, U., I. Zondervan, B. Rost, P. D. Tortell, and F. M. M. Morel. 2000. Reduced calcification of marine plankton in response to increased atmospheric CO₂. *Nature* **407**: 364–367. doi:10.1038/35030078
- Riegman, R., W. Stolte, A. A. M. Noordeloos, and D. Slezak. 2000. Nutrient uptake and alkaline phosphatase (ec 3:1:3:1) activity of *Emiliania huxleyi* (prymnesiophyceae) during growth under n and p limitation in continuous cultures. *J. Phycol.* **36**: 87–96. doi:10.1046/j.1529-8817.2000.99023.x
- Rosas-Navarro, A., G. Langer, and P. Ziveri. 2016. Temperature affects the morphology and calcification of *Emiliania huxleyi* strains. *Biogeosciences* **13**: 2913–2926. doi:10.5194/bg-13-2913-2016
- Rossi, S., and J.-M. Gili. 2007. Short-time-scale variability of near-bottom seston composition during spring in a warm temperate sea. *Hydrobiologia* **575**: 373–388. doi:10.1007/s10750-006-0390-y
- Rossi, S., and others. 2019. Changes of energy fluxes in marine animal forests of the Anthropocene: Factors shaping the future seascape. *ICES J. Mar. Sci.* **76**: 2008–2019. doi:10.1093/icesjms/fsz147
- Rossoll, D., R. Bermúdez, H. Hauss, K. G. Schulz, U. Riebesell, U. Sommer, and M. Winder. 2012. Ocean acidification-induced food quality deterioration constrains trophic transfer. *PLoS One* **7**: e34737. doi:10.1371/journal.pone.0034737
- Sailley, S., M. Vogt, S. Doney, and others. 2013. Comparing food web structures and dynamics across a suite of global marine ecosystem models. *Ecol. Model.* **261–262**: 43–57. doi:10.1016/j.ecolmodel.2013.04.006
- Schlüter, L., K. T. Lohbeck, M. A. Gutowska, J. P. Gröger, U. Riebesell, and T. B. H. Reusch. 2014. Adaptation of a globally important coccolithophore to ocean warming and acidification. *Nat. Clim. Chang.* **4**: 1024–1030. doi:10.1038/nclimate2379
- Seifert, M., B. Rost, S. Trimborn, and J. Hauck. 2020. Meta-analysis of multiple driver effects on marine phytoplankton highlights modulating role of pCO₂. *Glob. Chang. Biol.* **26**: 6787–6804. doi:10.1111/gcb.15341
- Sett, S., L. T. Bach, K. G. Schulz, S. Koch-Klavsen, M. Lebrato, and U. Riebesell. 2014. Temperature modulates coccolithophorid sensitivity of growth, photosynthesis and calcification to increasing seawater pCO₂. *PLoS One* **9**: e88308. doi:10.1371/journal.pone.0088308
- Shaltout, M., and A. Omstedt. 2014. Recent sea surface temperature trends and future scenarios for the Mediterranean Sea. *Oceanologia* **56**: 411–443. doi:10.5697/oc.56-3.411
- White, M. M., J. D. Waller, L. C. Lubelczyk, D. T. Drapeau, B. C. Bowler, W. M. Balch, and D. M. Fields. 2018. Coccolith dissolution within copepod guts affects fecal pellet density and sinking rate. *Sci. Rep.* **8**: 9758. doi:10.1038/s41598-018-28073-x
- Woodworth, B. D., R. L. Mead, C. N. Nichols, and D. R. J. Kolling. 2015. Photosynthetic light reactions increase total lipid accumulation in carbon-supplemented batch cultures of *Chlorella vulgaris*. *Bioresour. Technol.* **179**: 159–164. doi:10.1016/j.biortech.2014.11.098
- Ziveri, P., B. de Bernardi, K.-H. Baumann, H. M. Stoll, and P. G. Mortyn. 2007. Sinking of coccolith carbonate and potential contribution to organic carbon ballasting in the deep ocean. *Deep Sea Res. Part II Top. Stud. Oceanogr.* **54**: 659–675. doi:10.1016/j.dsr2.2007.01.006
- Zuur, A. F., E. N. Ieno, N. J. Walker, A. A. Saveliev, and G. M. Smith. 2009a. GLM and GAM for count data. Springer, p. 209–243.
- Zuur, A. F., E. N. Ieno, N. J. Walker, A. A. Saveliev, and G. M. Smith. 2009b. Meet the exponential family, p. 193–208. *In* A. F. Zuur, E. N. Ieno, N. Walker, A. A. Saveliev, and G. M. Smith [eds.], *Mixed effects models and extensions in ecology with R*. Springer.

Acknowledgments

This work was funded by the ASSEMBLE Plus grant program (Project 730984_A+), the Spanish Ministry of Science and Innovation, BIOCAL Project (PID2020-113526RB-I00) and CALMED project (CTM2016-79547-R). Roberta Johnson received a fellowship from MINECO (FPI/BES-2017-080469). This work is contributing to the ICTA “Unit of Excellence” (MINECO, MDM2015-0552; CEX2019-000940-M), and The Marine and Environmental Biogeosciences research group of the Generalitat de Catalunya (2017 SGR-1588). The authors would like to thank the specialized team at Station Biologique De Roscoff who helped us conduct the experiment. The authors would also like to thank the anonymous reviewers for their comments that helped to greatly enhance and refine the manuscript.

Conflict of interest

The authors declare that there is no conflict of interest.

Submitted 28 November 2021

Revised 25 March 2022

Accepted 03 August 2022

Associate editor: Susanne Menden-Deuer